First-Principle DFT and MP2 Modeling of Infrared Reflection−Absorption Spectra of Oriented Helical Ethylene Glycol Oligomers

Lyuba Malysheva,[†] Alexander Onipko,[‡] Ramūnas Valiokas,[§,||] and Bo Liedberg*[,§]

Bogolyubov Institute for Theoretical Physics, Kiev, Ukraine, Division of Physics, Luleå University of Technology, S-971 87 Luleå, Sweden, and Division of Molecular Physics, Department of Physics and Measurement Technology, Linköping University, S-581 83 Linköping, Sweden

Received: January 21, 2005; In Final Form: April 29, 2005

First-principle modeling is used to obtain a comprehensive understanding of infrared reflection absorption (RA) spectra of helical oligo(ethylene glycol) (OEG) containing self-assembled monolayers (SAMs). Highly ordered SAMs of methyl-terminated 1-thiaoligo(ethylene glycols) [$HS(CH_2CH_2O)_nCH_3$, $n = 5, 6$] on gold recently became accessible for systematic infrared analyses [Vanderah et al., *Langmuir*, **2003**, *19*, 3752]. We utilized the quoted experimental data to validate the first-principle modeling of infrared RA spectra of $HS(CH_2CH_2O)_{5,6}CH_3$ obtained by (i) DFT methods with gradient corrections (using different basis sets, including 6-311++G**) and (ii) HF method followed by a Møller−Plesset (MP2) correlation energy correction. In focus are fundamental modes in the fingerprint and CH-stretching regions. The frequencies and relative intensities in the calculated spectra for a single molecule are unambiguously identified with the bands observed in the experimental RA spectra of the corresponding SAMs. In addition to confirming our earlier assignment of the dominating peak in the CH-stretching region to CH_2 asymmetric stretching vibrations, all other spectral features observed in that region have received an interpretation consistent (but not in all cases coinciding) with previous investigations. The obtained results provide an improved understanding of the orientation and conformation of the molecular building blocks within OEG-containing assemblies, which, in our opinion, is crucial for being able to predict the folding and phase characteristics and interaction of OEG-SAMs with water and proteins.

Introduction

Solution self-assembly of oligo(ethylene glycol) (OEG)-containing compounds has developed into a very attractive surface modification strategy. It is used prominently by the biomaterial and bioanalytical communities, primarily because of the advantageous properties of such SAMs in contact with complex biological fluids. The exposed OEG segments demonstrate a variety of protein selective properties that have been thoroughly investigated during the past few years.[1−5] For example, very interesting relationships between the conformational characteristics of the OEG segments and the protein rejecting properties have been observed.[1,5] The OEG segments also serve as efficient linkers and/or hydrogel cushions for the tethering of lipid bilayer assemblies.[6] Moreover, the OEG segments display very interesting structural properties. The ability to control and manipulate the conformation of the segments (e.g., into helical and all trans) by varying the oligomer chain length[4] and/or the lattice parameters of the supporting substrate[3] offers a convenient way to design new materials with unique surface properties. Characterization of the OEG surface structure and conformation is mostly inferred from infrared reflection absorption (RA)[1,3−5,7] and IR-visible sum frequency vibrational spectra.[8,9] The contribution of OEG to the SAM spectra is usually interpreted referencing the theoretical and experimental investigation of ethylene glycol polymers by Miyazawa et al.[10] and the infrared spectrum of the folded-chain crystal polymorph of crystalline poly(ethylene oxide).[11] Although, a fairly good comprehension has been achieved, we are still quite far from complete understanding of the infrared spectrum of OEG-containing SAMs. The CH_2-stretching region (~2700−3100 cm^{-1}), for example, is especially difficult to interpret because of several strong and partly overlapping bands representing the symmetric and asymmetric vibrations of CH_2 (methylene) groups of the alkane and OEG portions, respectively.[3,4] The two side peaks are commonly recognized as the alkane chain contribution to the spectrum,[3,4,8] Figure 1b, and the central peak, seen at 2893 cm^{-1}, has been assigned as the *symmetric* CH_2-stretching vibration characteristic for the helical OEG conformation (see, e.g., refs 3 and 10). In attempt to validate the assignments of OEGs, DFT-LSDA modeling of RA spectra was performed in our laboratories for an optimized helical conformation of $H(CH_2CH_2O)_nH$, $n = 4−7$.[7] Ab initio calculations supported by physical arguments led us to the conclusion that the band in focus is mostly due to *asymmetric* CH_2-stretching modes of a helical OEG chain.

One of the reference spectra used in that modeling is shown in Figure 1. It was obtained for a SAM based on the commercially available PEG750 compound, whose structure is $HS(CH_2)_2CONH(CH_2CH_2O)_{15}CH_3$ (abbreviated $(EG)_{15}CH_3$−SAM). The main contribution to RA spectrum of this SAM originates from the methoxy-terminated ethylene glycol (EG) portion. The other reference spectrum used in ref 7 was obtained for a SAM of $HS(CH_2)_{15}CONH(CH_2CH_2O)_6H$ (not shown).

* Corresponding author. Fax: 46 (0)13 288969; Tel: 46 (0)13 281877; E-mail: bolie@ifm.liu.se

[†] Bogolyubov Institute for Theoretical Physics.

[‡] Luleå University of Technology.

[§] Linköping University.

[||] Present address: Molecular compounds physics laboratory, Institute of Physics, Savanoriu 231, LT-02300 Vilnius, Lithuania.

10.1021/jp0503765 CCC: $30.25
Published on Web 06/16/2005

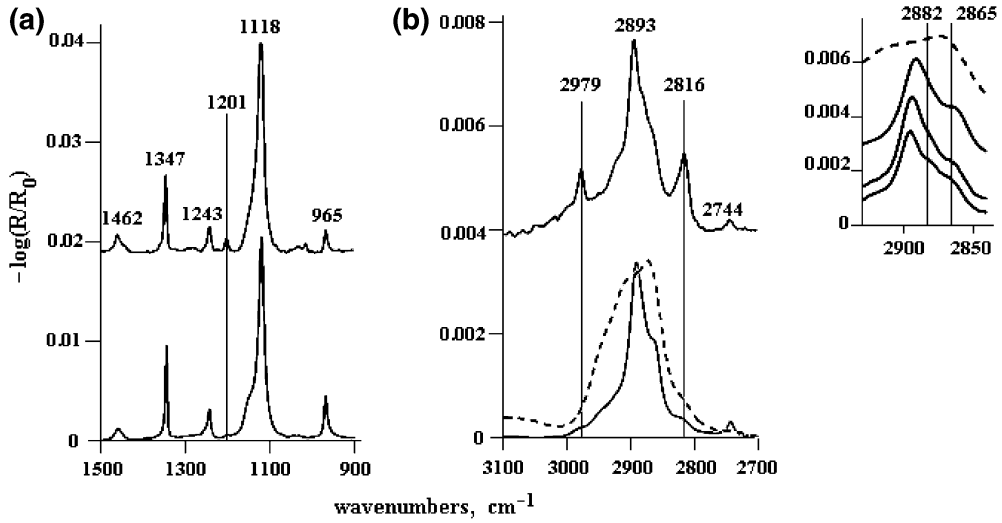

Figure 1. Experimental RA spectra in the fingerprint (a) and CH-stretching (b) regions. Upper part represents a RA spectrum of self-assemblies of $HS(CH_2CH_2O)_5CH_3$,[1] abbreviated as $(EG)_5CH_3$ SAM. The lower part displays a RA spectrum of an $EG_{15}CH_3$ SAM,[7] see text. The band intensity in latter spectrum is scaled by factor 3 to account for the chain length difference between the two compounds. Dashed line shows the spectrum of the $(EG)_{15}CH_3$ compound obtained in a pressed KBr pellet. Inset represents (from bottom to top) spectra of $(EG)_5CH_3$ SAM,[1] $(EG)_6CH_3$ SAM,[1] $(EG)_{15}CH_3$ SAM,[7] and the $(EG)_{15}CH_3$ compound in a pressed KBr pellet.

These were the best experimental spectra available at that time to compare with all-electron ab initio modeling. Strictly speaking, neither of the experimental spectra was perfectly suitable for the purpose of comparison with the calculated spectra because of presence of alkyl and amide groups. Thus, the RA spectrum of $(EG)_{15}CH_3$ SAM can be regarded as representative of the OEG spectrum only to the first approximation. It is even more difficult to identify the OEG contribution in the CH_2-stretching region for SAMs containing long alkyl chains. In general, the use of DFT-LSDA has proven to be practical and instrumental in microscopic interpretation of observed RA spectra. Certain limitations of the method, however, have left room for questioning the reproducibility of more subtle features, such as the shoulder structure observed in the band with the maximum at 2893 cm^{-1} and others.

Very recently, highly ordered self-assemblies of methyl-terminated 1-thiaoligo(ethylene glycols) [$HS(CH_2CH_2O)_nCH_3$, $n = 5, 6$], have been obtained and characterized by RA spectroscopy and other methods.[1,5] The RA spectra of the $(EG)_5CH_3$ SAM and $(EG)_{15}CH_3$ SAM are compared in Figure 1. At first glance, these spectra look almost identical, except for the three bands indicated by vertical lines at 1201, 2816, and 2979 cm^{-1}, respectively. The marked bands correspond to modes involving CH_3 group vibrations,[1] and the increase in relative intensities of these bands in the RA spectrum of the $(EG)_5CH_3$ SAM is in line with the expected relative occurrence of CH_3 groups in the two compounds.

In this work, the spectra represented in Figure 1 are used for comparison with model RA spectra of helical $HS(CH_2CH_2O)_n$-CH_3, $n = 5, 6$, with the helical axis aligned perpendicularly to the metal surface. Our choice of the helical molecular conformation is supported by the fact that model spectra of $HS(CH_2$-$CH_2O)_{5,6}CH_3$ with one or several trans units (not shown here) do not agree with experimental results. There are also many other experimental and theoretical arguments in favor of helical OEG-geometry in $(EG)_{5,6}CH_3$ SAMs and related self-assemblies, see refs 1, 3−5, 7 and references therein.

So far, ab initio methods have been used in studies of substantially shorter molecules. HF calculations of the optimized geometry of the diglyme molecule ($H_3C(OCH_2CH_2)_2OCH_3$) and its conformers were performed in ref 12. Conformational energies of the DME molecule ($H_3COCH_2CH_2OCH_3$) and its vibrational frequencies were reported at the HF level[13] only for the fingerprint region. The energies of different conformations of OEG molecules (of the type $(OCH_2CH_2)_nO-Me$, $n = 1-4$) and their interaction with water were investigated in detail in ref 14 on the basis of the DFT methods. The MP2 method has been used for calculations of vibrational frequencies in the CH-stretching range of 2-methoxy ethanol $HO(CH_2CH_2O)CH_3$.[15] However, the BP86 and MP2 methods have never been tried for modeling RA spectra of real OEG-containing SAMs. Thus, our main focus was to discover to what extent the calculated ab initio spectrum of $HS(CH_2CH_2O)_nCH_3$ [denoted below as $(EG)_nCH_3$] could reproduce experimental RA spectra of $(EG)_nCH_3$ SAMs, specifically, those that are shown in Figure 1.

Details of Calculations

In ab initio modeling of infrared RA spectra, the choice of method is crucial and always questionable. Therefore, we compare the results obtained by different methods. The optimization of the molecular geometry and calculations of vibrational frequencies and transition dipole moments (TDMs) were performed using the G03 package of programs with the LSDA/3-21G* (for comparison to our previous study[7]), BP86 exchange-correlation functional utilizing two different basis sets (6-31G* and 6-311++G**), and with HF method followed by a Møller−Plesset correlation energy correction (MP2/6-31G*). The data obtained by the latter method have been scaled. Namely, the calculated frequencies in the fingerprint and CH-stretching regions are multiplied by 0.947 and 0.934, respectively, see Figures 2 and 3. In contrast, all frequencies obtained by different DFT methods are presented here without any scaling. This is a clear advantage because large and complex molecular assemblies consisting of different components can be modeled in a similar way (ongoing work). The B3LYP exchange-correlation functional gives a spectrum that is very similar to that obtained with BP86 method. However, the B3LYP method tends to shift the peaks to higher frequencies than those observed for the BP86 method.

To simulate the RA spectrum for the given orientation of molecule $(EG)_nCH_3$ with respect to the SAM-supporting metal

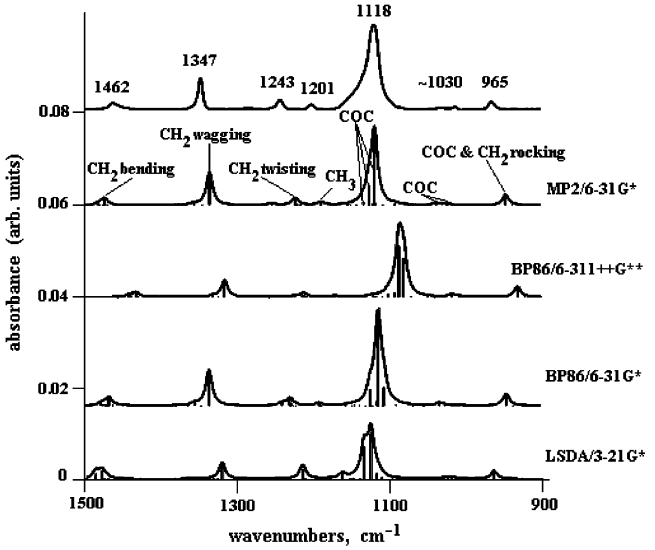

Figure 2. Experimental and calculated RA spectra in the fingerprint region. Upper curve represents the RA spectrum of the $(EG)_5CH_3$ SAM.[1] The single-molecule $(EG)_5CH_3$ spectra (oligomer helix axis is perpendicular to the SAM surface) are calculated with the use of (from bottom to top) LSDA/3-21G*, BP86/6-31G*, BP86/6-311++G**, and MP2/6-31G* method/basis sets, respectively. Lorentzian-shaped peaks (HWHM = 5 cm^{-1}) are centered at the fundamental mode frequency, and the corresponding values of $(TDM_z)^2$ are indicated by vertical bars. The scaling factor used for the MP2 method equals 0.947. The assignments of the fundamental modes in the calculated spectra using the three other methods are the same as that obtained by MP2/6-31G*.

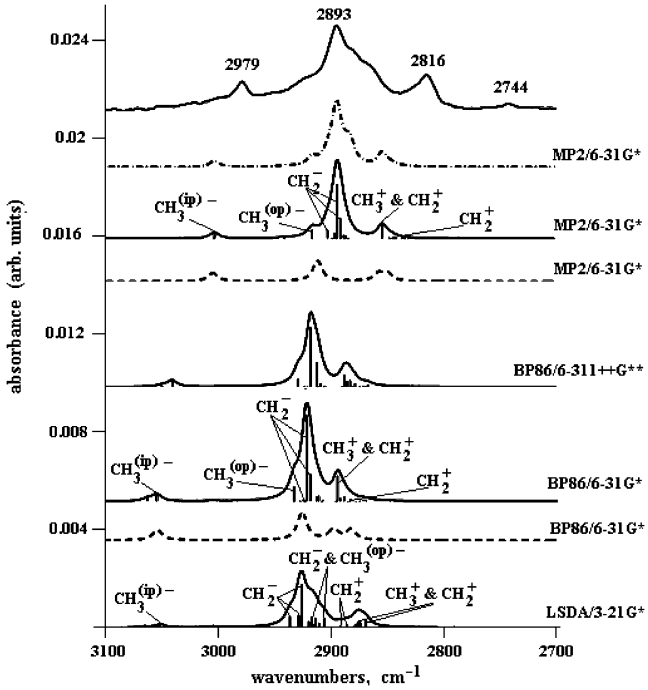

Figure 3. Experimental and calculated spectra in the CH-stretching region. Upper solid curve represents the RA spectrum of the $(EG)_5CH_3$ SAM.[1] Solid lines: the single-molecule $(EG)_5CH_3$ spectra (oligomer helix axis is perpendicular to the SAM surface) are calculated with the use of (from bottom to top) LSDA/3-21G*, BP86/6-31G*, BP86/6-311++G**, and MP2/6-31G* method/basis sets, respectively. Scaling factor equals 0.934 for the curves calculated with MP2 method; all other model spectra are unscaled. Dash dotted line: $(EG)_5CH_3$ spectrum calculated with the use of MP2/6-31G* and additional scaling of one mode by 0.997 (see text). Dashed lines: the averaged spectrum of dimethyl ether calculated with the help of MP2/6-31G*(upper curve) and BP86/6-31G* (lower curve). Lorentzian-shaped bands (HWHM = 5 cm^{-1}) are centered at the fundamental mode frequency; the corresponding values of $(TDM_z)^2$ are indicated by vertical bars. The assignments of the fundamental modes for the spectra calculated by BP86/6-311++G** and BP86/6-31G* are the same.

surface, the output of transition dipole moments needs to be recalculated to obtain the TDM components in the molecular coordinates. This procedure allows us to find the TDM projections on the laboratory coordinate axes (commonly chosen so that the *xy*-plane coincides with the substrate surface[16,17]) for arbitrary values of the tilt, twist, and azimuthal angles that determine the molecular orientation. The molecular *z*-axis coincides with the helical axis. The latter has been assumed to be normal to the substrate surface, meaning that only *z* TDM component contributes to the absorption (metal−surface selection rule). The model spectra were obtained in the dipole approximation, as the sum of Lorentsian-shaped peaks, each centered at the fundamental mode frequency and having the half width at half-maximum (HWHM) indicated in Figures 2 and 3. Peak heights are proportional to the squared TDM's *z* component of the corresponding mode.

Results and Discussion

A. Fingerprint Region (900−1500 cm^{-1}). Figure 2 compares the observed RA spectrum of the $(EG)_5CH_3$ SAM[1] in the fingerprint region with four model RA spectra. Calculations were carried out by the LSDA/3-21G*, BP86 method with two different basis sets and by MP2/6-31G* for a single molecule of $(EG)_5CH_3$ and $(EG)_6CH_3$, respectively. Here, we do not show experimental and calculated spectra of the $(EG)_6CH_3$ SAM, which are very similar to those of the $(EG)_5CH_3$ SAM, except for small differences in band intensities.

The well-established assignment of the characteristic bands in the fingerprint region for unidirectional ethylene glycol oligomers is as follows:[1,3−5,7] asymmetric COC stretching + CH_2 rocking (965 cm^{-1}), asymmetric COC stretching (1118 cm^{-1}), CH_2 twisting (1243 cm^{-1}), CH_2 wagging (1347 cm^{-1}), and CH_2 bending (scissoring) (1462 cm^{-1}). These calculations identify a small peak at 1201 cm^{-1} as a manifestation of local wagging−rocking CH_3 vibrations, where the wagging component corresponds to the out-of-plane hydrogen atoms (see definitions of out-of-plane (op) and in-plane (ip) CH_3 hydrogen atoms/vibrations in refs 16 and 18). Furthermore, the weak structure centered at ∼1030 cm^{-1} (experimental curve) is also reproduced in all calculated spectra at nearly the same position. It corresponds to asymmetric COC stretching vibrations (the most intense mode is placed at 1033 cm^{-1} by BP86/6-31G* method), and thus it has the same origin as the dominant peak in the region.

All methods used are quite good in reproducing the relative positions and intensities of the bands observed for the $(EG)_nCH_3$ SAMs in this spectral region.[1] The absolute frequency values are within 6% for MP2 spectrum (unscaled), while other methods reproduce the experimental data within 2%. A close similarity between the calculated single-molecule spectra for $(EG)_nCH_3$ and the experimental RA spectra of related SAMs suggests that, in the fingerprint region, the observed spectral regularities are mostly governed by the intramolecular interactions.

All methods indicate a pronounced multimode structure of the dominating band at 1118 cm^{-1}. The number of contributing modes (shown by vertical bars with the height proportional to $|TDM_z|^2$), their relative intensity, and position depend, however, on the method and basis set used. The 1118 cm^{-1} band has a noticeable asymmetry with a high-frequency shoulder that is well resolved in the $(EG)_{15}CH_3$ SAM spectrum, see Figure 1a.

This asymmetry is frequently attributed to the presence of nonhelical conformations, since all-trans and amorphous OEGs are expected to have a strong band in the 1120−1150 cm^{-1} region.[3−5] However, the observed shoulder may well be just an inherent property of the given band taking into account its multimode structure revealed in our calculations, Figure 2. Indeed, a few cm^{-1} shift of the high-frequency satellite mode in the MP2- or BP86/6-31G* representation of the COC band would make its shape practically indistinguishable from that observed experimentally. Note also that the intensity and frequency of contributing modes, in general, are dependent on the OEG chain length. This may be the reason for small changes in the COC band appearance seen in Figure 1a for two SAMs containing different number of ethylene glycol units. Thus, regardless of whether the above interpretation reflects reality or not, the presence of a multimode structure in the COC band contradicts the asymmetry argument as evidence for conformational disorder within OEG SAMs.

B. CH-Stretching Region (2700−3100 cm^{-1}). The experimental RA spectrum in the CH-stretching region for the $(EG)_5CH_3$ SAM (same as in Figure 1) is compared with calculated spectra using different methods for $(EG)_5CH_3$ in Figure 3. The nature of the observed spectral features and their reproducibility in the calculations is discussed, starting with the low-frequency band at 2744 cm^{-1}.

Band at 2744 cm^{-1}. This weak band was assigned by Miyazawa et al.[10] to a combination of CH_2 twisting + bending modes. A band of similar intensity at approximately the same position is always observed in the RA spectra of helical OEG-containing SAMs (cf. Harder et al.[3] and Svedhem et al.[19]). However, combination modes are not reproduced in our calculations, which are based on the first-order perturbation theory. Hence, all nonlinear excitations are left beyond the scope of such modeling. It is worthwhile noting, however, that our calculated spectra reveal a CH_2 twisting vibration at 1272 cm^{-1} and two CH_2 bending vibrations at 1469 and 1471 cm^{-1} (the frequencies are taken from the BP86/6-31G* spectrum), respectively. According to ref 10, just these fundamental modes (which are not seen in the calculated spectra in Figure 2, because of their weak *z* TDM components) may be responsible for the appearance of CH_2 twisting+bending band: 1272 + 1469 = 2741 cm^{-1} and 1272 + 1471 = 2743 cm^{-1}.

Band at 2816 cm^{-1}. This band is commonly assigned to symmetric CH_3-stretching[1,3,8] (referred below as CH_3^+ vibrations). The shape and position of this band are known to depend on the nature of the substituent to which the methyl group is attached. For example, in spectra of dimethyl ether, a doublet is observed with frequencies at 2819/2826 cm^{-1}.[20] A similar doublet at 2810/2828 cm^{-1} was reported for SAMs of methoxyhexadecanethiols.[18] It is instructive therefore to summarize data on characteristic vibrations of end CH_3-groups in CH_3OCH_3, $(EG)_5CH_3$, and $HS(CH_2)_{16}OCH_3$ molecules, Table 1. This also gives a useful cross-check of the calculation methods exploited in our work.

Table 1 shows measured and calculated frequencies of CH_3^+ doublet in CH_3OCH_3 and in SAMs of $HS(CH_2)_{16}OCH_3$. Note also that the frequency of the band associated with CH_3^+ vibrations in $(EG)_nCH_3$ SAMs is practically the same for n = 5 and n = 15, see Figure 1. Corresponding data are also given for asymmetric CH_3-stretching vibrations which are labeled in Figure 3 and listed in Table 1; they are henceforth denoted as $CH_3^{(op)-}$ and $CH_3^{(ip)-}$. Indexes op (= out of plane) and ip (= in plane) refer to C−H bonds lying, respectively, out of and in the COC plane. Out-of-plane and in-plane C−H bonds are not equivalent to one another.[18,21] Therefore, they give rise to vibrations of different frequencies; the $CH_3^{(ip)-}$ vibration, which mostly involves the in-plane C−H bond, appears at the highest frequency.

TABLE 1: Comparison of Experimental and Calculated Frequencies of Fundamental Methyl Modes for Dimethyl Ether, $(EG)_5CH_3$, and $HS-(CH_2)_{16}-O-CH_3$

	Frequencies of fundamental modes (cm^{-1})			
	$\nu_+(CH_3^+)$	$\nu_{op}(CH_3^{(op)-})$	$\nu_{ip}(CH_3^{(ip)-})$	Δ^a
CH_3-O-CH_3[20]	2819/2826	2928	2989/2993	170/167
BP86/6-31G*	2883/2899	2927	3056/3058	173/159
BP86/6-311++G**	2876/2889	2922	3043/3044	167/155
MP2/6-31G* (scaling factor = 0.934)	2849/2856	2911	3004/3005	155/149
$(EG)_5CH_3$[1]	2816	~2920	2979	163
BP86/6-31G*	2895	2934	3056	161
BP86/6-311++G**	2888	2929	3041	153
MP2/6-31G* (scaling factor = 0.934)[b])	2854	2917	3004	150
$HS-(CH_2)_{16}-O-CH_3$[18]	2810/2828	2930	2981	171/153
BP86/6-31G*	2863/2893	2930	3053	190/160

[a] $\Delta = \nu_{ip} - \nu_+$ is the difference between frequencies of symmetric and asymmetric (in-plane) modes text. [b] Frequencies of these modes obtained by MP2/6-31+G* for 2-methoxy ethanol molecule[15] are practically the same (2852 cm^{-1}, 2917 cm^{-1}, 3004 cm^{-1} with our scaling).

In dimethyl ether (C_{2v} point group symmetry), the CH_3^+ doublet vibrations can be classified into A_1 (high frequency) and B_1 (low frequency) species. Visually, in A_1 type of vibrations, C−H bond lengths in two CH_3 groups are changing in phase (in-phase vibrations). Whereas in B_1 type of vibrations, when C−H bonds shorten in one CH_3 group, they become longer in the other and vice versa (anti-phase vibrations). The same terminology is applicable to the $CH_3^{(ip)-}$ doublet, where in-phase asymmetric vibrations also appear at higher frequencies than anti-phase vibrations. Similarly, $CH_3^{(op)-}$ asymmetric vibrations form a doublet, but because of the molecular symmetry, only one of the components is observed in the infrared spectrum at 2928 cm^{-1}.[20]

The symmetry considerations used above are not applicable for the molecule of methoxyhexadecanethiol. Nevertheless, as is seen from Table 1, both experiment and calculations indicate that in this molecule there exists a CH_3^+ doublet at close frequencies, pointing out similarity of the doublet nature. Visualization of the vibrations in the calculated spectra shows that the components of the CH_3^+ doublet in $HS(CH_2)_{16}OCH_3$ correspond to in-phase and anti-phase symmetric vibrations of CH_3 group and the nearby CH_2 group (connected via oxygen), with the latter playing the role of the second CH_3 group in dimethyl ether. Again, the higher and lower frequencies represent, respectively, in-phase and anti-phase CH_3^+ -CH_2^+ vibrations. Note that in the original paper,[18] the authors attributed the assumed low-frequency component of the doublet to Fermi-resonance.

As it follows from the present calculations and in agreement with the experimental data, the doublet structure of the CH_3^+ band observed for dimethyl ether and methoxyhexadecanethiol disappears in $(EG)_nCH_3$ SAMs where CH_3-stretching symmetric vibrations reveal themselves as a band peaking at 2816 cm^{-1}, indicating one dominating mode and a number of smaller contributions. Similar to experiment, in all calculated spectra, this band appears as a low-frequency sideband of the main peak but shifted toward higher frequency with respect to its true position. Nearly the same shift as for CH_3^+ is obtained (by all methods) for the high-frequency sideband at 2979 cm^{-1} which associates with $CH_3^{(ip)-}$, see Table 1 and Figure 3. The blue

shift of CH_3^+ and $CH_3^{(ip)-}$ bands given by the BP86 method is about 70−80 cm^{-1}. Note that this corresponds to the reproducibility of experimental results with an accuracy that is better than 3%. The absolute values of all characteristic frequencies in the region are overestimated (up to 7−8%) by the MP2 method, but it gives still the same relative positions of the CH_3^+, $CH_3^{(op)-}$, and $CH_3^{(ip)-}$ bands that agree well with the corresponding bands observed in the experimental spectrum.

The calculated spectra noticeably diverge in the representation of the internal structure of the CH_3^+ band. In BP86/6-31G* and MP2/6-31G* spectra, this band appears essentially, as a single-mode band, whereas the LSDA/3-21G* and BP86/6-311++G** methods indicate a multimode composition of the band. Visualization of molecular vibrations shows that MP2 calculations predict a single localized mode, but the BP86 method suggests a high degree of delocalization of one or several modes of mixed CH_3^+/CH_2^+ character. Such a diversity in the predictions of the different ab initio methods seems, at first glance, to be connected with the above-mentioned systematic misplacement of frequencies of interrelated CH_3^+ and $CH_3^{(ip)-}$ vibrations. Because of this (method-caused) shift, CH_3^+ vibrations happen to occur within the region of the CH_2-stretching modes. As a consequence, favorable conditions are created for effective interaction and mixing of CH_3^+ and CH_2^+ vibrations. This results in the appearance of delocalized, mixed CH_3^+/CH_2^+ modes exposed in BP86 model spectra.

The most pertinent experimental data[1,3,18,20] suggest that the characteristic frequencies of the CH_3^+ vibrations appear at significantly lower frequencies than the majority of the CH_2^+ modes of the helical OEG chain, and that the overlap between the end group and chain vibrations should be rather small. In support of this statement, we notice that the spacing between the spectral position of the maximum and the shoulder (or vaguely resolved low-intensity maximum) in the observed spectrum of PEG750 in KBr (Figure 1) is about ∼40 cm^{-1}. We believe that these two features can be attributed to the dominating CH_2^- and CH_2^+ chain modes, which have comparable intensities in the averaged spectrum. Such an assumption agrees well with our calculations. For instance, BP86/6-31G* gives several CH_2^+ vibrations with large *x* and *y* TDM components within the interval 2885−2896 cm^{-1}, whereas the CH_2^- band maximum is placed at 2923 cm^{-1}, i.e., about 30−40 cm^{-1} higher. On the other hand, as is documented in many experiments, the dominating modes associated with characteristic vibrations of the CH_3 group attached to oxygen in different molecules such as methoxyhexadecanethiol and oligo(ethylene glycol) absorb at a position that is very close to that which they have in a molecule of dimethyl ether. Our calculations are consistent with this observation [compare spectral curves for dimethyl ether represented by dashed lines in Figure 3, and those obtained for $(EG)_5CH_3$]. Moreover, the frequency of $CH_3^{(op)-}$ vibration and frequency difference Δ between $CH_3^{(ip)-}$ and CH_3^+ vibrations, calculated within the framework of BP86 method, are in very good agreement with experimental data. We can, with certainty, conclude that the relative positioning of calculated frequencies of CH_3^+ and $CH_3^{(ip)-}$ vibrations with respect to the $CH_3^{(op)-}$ frequency is misplaced already for dimethyl ether by approximately ∼70−80 cm^{-1}. Hence, the required red shift to restore the correct position of the sidebands CH_3^+ and $CH_3^{(ip)-}$ in the calculated spectra is larger than the spacing between dominant CH_2^- and CH_2^+ chain modes (see above). With these observations in mind we can conclude that the band observed at 2816 cm^{-1} in the $(EG)_nCH_3$ SAM spectra appears near the low-frequency edge of the region of CH_2^+ chain modes and that, most likely, it is formed by a set of *localized* modes involving symmetric vibrations of CH_3 group and the nearby CH_2 group. Under perpendicular orientation of the helical (*z*) axis to the SAM surface, contribution of CH_2^+ modes to the apparent band intensity is negligible because of small *z* TDM components of this type of vibrations.[7] Calculations of TDMs for mixed CH_3^+/CH_2^+ modes show a dominating contribution from the CH_3^+ vibrations. The observed asymmetry of the band at 2816 cm^{-1} indicates a larger number and/or intensity of CH_3^+/CH_2^+ modes to the high-frequency side of the band maximum and, probably, some contribution of combination modes.[22]

Band at 2893 cm^{-1}. The main peak of this most intense broad band is reasonably reproduced by all the methods used. The BP86/6-31G* method, for example, gives the frequency of the band maximum with ∼1% accuracy. In our previous study,[7] the CH_2^- nature of the peak was demonstrated in the LSDA/3-21G* calculations of ethylene glycol oligomers $H(CH_2-CH_2O)_nH$. It was also shown that because the orientation of their TDMs is "unfavorable" (perpendicular to the helix axis), the CH_2^+ modes cannot create intense bands. That principal conclusion is fully supported by present modeling, which involves much more advanced methods/basis sets. (As mentioned, in many works the peak in focus was erroneously assigned to CH_2^+ vibrations.[3,4,10,22]) While ab initio calculations and subsequent analysis of TDMs of fundamental modes leave no doubt about CH_2^- origin of the band maximum, the shape obtained in the model spectra in that region does not seem to suggest straightforward interpretation of prominent band asymmetry or shoulder structure that is observed in experimental spectra. This is to be discussed next.

Shoulder at ∼2865 cm^{-1}. First, we focus at the low-frequency shoulder which in the experimental spectrum of the $(EG)_5CH_3$ SAM, shows up as a doublet feature (see Figure 1) indicating a likely presence of unresolved bands of lower intensity within the region of 2850−2890 cm^{-1}. However, according to the experiment,[1] the doublet merges into a single feature in the spectrum of the $(EG)_6CH_3$ SAM (see inset in Figure 1), which makes it very similar in appearance to the low-frequency shoulder at ∼2865 cm^{-1} in the spectrum of $(EG)_{15}CH_3$ SAM. The resemblance of this feature to that in the calculated LSDA spectrum should be regarded as accidental because it does not appear in similar calculations for the $HO(EG)_nH$ molecule.[7] None of the other model spectra reveal any superimposed structure, showing instead a monotonic decrease of the band intensity due to decrease in TDMs of asymmetric stretching vibration modes (see BP86 and MP2 spectra depicted in Figure 3). Earlier,[7] we have tried to explain the difference in the main-band shape as it appears in observed and ab initio modeled spectra by assuming a tilt of the helical axis of OEG molecules within SAMs. For clear reasons, tilting the helix axis with respect to the SAM normal should increase the contribution of CH_2^+ stretching modes in the band formation. It was found, however, that even at a tilt as large as 20 degrees, though it results in appearance of a shoulder on the low-frequency side of CH_2^- band, the intensity of the appearing band is too low to be consistent with experimental results.

The model spectra shown in Figure 3 reveal a differently shaped main band, suggesting that the band shape is strongly dependent on the number, relative intensity, and position of main contributing modes. Neither of the existing ab initio methods can pretend to reproduce the delicate interplay of these factors with a one-to-one correspondence. At the same time, for the region of interest, even relatively small changes in TDMs and spacing of CH_2^- modes may result in quite substantial changes

of the band shape. The spectrum shown by the dashed dotted line in Figure 3 serves as an example: the low-frequency shoulder of the main band would be reproduced by the MP2 model spectrum, if spacing between the two most intense modes were ~10 cm^{-1} larger. It is also easy to imagine that just a small intensity redistribution between CH_2^- modes can give a shoulder structure in BP86 spectra similar to that obtained by the LSDA method. These simple arguments show that the shoulder at 2865 cm^{-1} can be due to contribution of asymmetric CH_2-stretching vibrations. At least, there is no reason to rule out such a possibility.

A similar spectral feature at a close frequency was interpreted as a parallel band (that is a band observed under parallel orientation of electric field with respect to the helical axis) for high polymers of ethylene glycol in crystalline films.[10] Miyazawa et al. assigned the band at 2865 cm^{-1} to combination vibrations, which also can be regarded as a plausible explanation. By using the same symmetry arguments as those in ref 10, we identified suitable candidates to be the two vibrations with frequencies (according to BP86/6-31G* method) 1421 cm^{-1} (wagging) and 1469 cm^{-1} (bending), both of *E* symmetry. In ref 10, these vibrations are observed at 1415 and 1470 cm^{-1}, respectively. The corresponding combination mode gives rise to a parallel band at 2890 cm^{-1}. Since the maximum of the main band (calculated by the same method) is at 2923 cm^{-1}, we obtained quite convincing agreement with the calculated (33 cm^{-1}) and observed (28 cm^{-1}) spectral separation between the main peak and low-frequency shoulder. As a rule, however, combination modes are disguised in RA spectra by fundamental modes having close frequencies and larger intensity, unless the former are enhanced by an intense fundamental mode via the Fermi-resonance mechanism. Because in the region 2860−2950 cm^{-1}, only CH_2^- vibrations may have large *z* TDM components, the shoulder at 2865 cm^{-1} can be attributed to Fermi resonance between one or a few CH_2 stretching asymmetric modes and a combination of deformation modes.

Shoulder at ~2920 cm^{-1}. To assign this feature, we shall refer to the methyl characteristic vibrations (CH_3^+, $CH_3^{(op)-}$, and $CH_3^{(ip)-}$) that we discussed in conjunction with the sideband at 2816 cm^{-1}. According to our calculations and in agreement with experiment, these vibrations are shown to have very close (within ~10 cm^{-1} range) frequencies in the spectra of dimethyl ethers, methoxyhexadecanethiols, and methyl/thiol-terminated oligo(ethylene glycols). Both BP86 and MP2 methods place the $CH_3^{(op)-}$ frequency about 40 cm^{-1} above the most intense CH_2^- mode. Both predict the appearance of a high-frequency shoulder. The relative position of the shoulder with respect to the dominating maximum, agrees very well with the one that is observed experimentally (see Figure 3). These data allow one to assign the shoulder observed in the spectra of $(EG)_nCH_3$ SAMs at approximately 2920 cm^{-1} to methyl out-of-plain asymmetric vibrations. The frequency of the (dominating) $CH_3^{(op)-}$ mode in $HS(EG)_{5,6}CH_3$, calculated by BP86 exchange-correlation functional, is 2934 and 2929 cm^{-1}, respectively given by 6-31G* and 6-311++G** basis sets. Visualization of BP86 and MP2 spectra shows a local character of the $CH_3^{(op)-}$ mode in $HS(EG)_{5,6}CH_3$ molecules (similar result is obtained for $HS(CH_2)_{16}OCH_3$ molecules). The assignment of the high-frequency shoulder to vibrations of the CH_3 group is also supported by an observed decrease in the relative intensity of this spectral feature for SAMs containing longer ethylene glycol chains (see Figure 1b). In sum-frequency spectra of methyl-terminated hexadecanethiols, the $CH_3^{(op)-}$ vibrations are observed as a separate band peaked at 2930 cm^{-1}.[16] This is very close to the frequency obtained by BP86 method for the $CH_3^{(op)-}$ mode (Table 1).

Band at 2979 cm^{-1}. Similar to the sideband at 2816 cm^{-1} (dominated by CH_3^+ vibrations) and main-band shoulder at 2920 cm^{-1} (dominated by $CH_3^{(op)-}$ vibrations), the origin of a high-frequency sideband at 2979 cm^{-1} can be traced to the $CH_3^{(ip)-}$ doublet 2993/2989 cm^{-1} in dimethyl ether.[20] According to BP86/6-31G* calculations for this symmetric molecule (see Table 1 and dashed-line spectrum in Figure 3), two frequencies of the doublet correspond to in-phase (3058 cm^{-1}) and anti-phase (3056 cm^{-1}) large-amplitude stretching/contraction motion of in-plane C−H bonds. Mode analysis and visualization of calculated vibrational spectra for $HS(CH_2)_{16}OCH_3$ and $HS(EG)_{5,6}CH_3$ show that in SAMs of these molecules, only one local mode survives which involves an intense localized $CH_3^{(ip)-}$ vibration. In all calculated spectra represented in Figure 3 (the last to the left), the $CH_3^{(ip)-}$ band has a two-mode structure with another much weaker mode corresponding to asymmetric vibrations of the CH_2 group near the sulfur atom.

As is emphasized in the discussion of the nature of CH_3^+ band, all methods that we used give higher frequencies than those experimentally observed for $CH_3^{(ip)-}$ and CH_3^+ modes. (Interestingly, regardless of the method, the frequency shift preserves unaffected spacing between the modes.) At the same time, the relative position of other stretching vibration modes ($CH_3^{(op)-}$, CH_2^-, and CH_2^+) is obtained reasonably close to those seen in experiment. The observed relative intensities of the bands at 2816, 2893, and 2979 cm^{-1} and shoulder at 2920 cm^{-1} are also satisfactorily reproduced. Hence, just a red shift of $CH_3^{(ip)-}$ and CH_3^+ bands by about 70−80 cm^{-1} would make the observed spectrum of $(EG)_nCH_3$−SAM well recognizable in our model spectra of $HS(EG)_nCH_3$. However, even with such a correction, reproducibility of fine details of the spectrum is beyond the capabilities of ab initio methods available in the G03 package of programs.

In addition to the inherent method drawbacks in representation of the fundamental modes, the main sources of discrepancy between the experimental RA spectra and calculated spectra are due to the following computational restrictions: (i) only fundamental excitations contribute to the spectrum and (ii) the single-molecule approximation. As to the latter, our calculations provide a consistent explanation to all spectral features in the SAM RA spectra. The limited reproducibility in the CH-stretching region has, most likely, other roots which are discussed above. However, we cannot see any reason why weak, mostly van der Waals type of intermolecular interactions could affect significantly the appearance of the single-molecule spectrum governed by far stronger intramolecular interactions.

The quantitative description of nonlinear effects such as combined vibrations and Fermi resonances goes far beyond the scope of this work. To be able to address these unresolved problems, it seems useful to have a clear understanding of the feasibilities of ab initio methods in describing RA spectra at a somewhat simplified level. In this respect, a number of "methodological" comments have been made regarding the three most common ab initio methods. The question, which of these three methods of calculations is preferable, seems to have no conclusive answer. Table 1 compares the results of MP2 and BP86 calculations with observed frequencies of CH_3 group vibrations. Although after scaling, MP2 data are in somewhat better agreement with experiments, this is a gain that hardly justifies a huge increase in computational time. On the other hand, the LSDA method suggests a multimode structure of the main band in CH stretching region, which is not consistent with

experimental observations. Thus, experience of this study recommends the BP86/6-31G* method as most suitable for ab initio analysis of structure and vibration properties of the given oligomer family.

Concluding Remarks

Ab initio modeling of RA spectra of monolayer self-assemblies of methyl-terminated helical ethylene glycol oligomers on gold was performed here using DFT methods with gradient corrections and by the HF method followed by a Møller−Plesset (MP2) correlation energy correction. Modeling is based on a perpendicular orientation of the helical axis to the substrate surface and a single-molecule approximation assuming that intermolecular interactions within the SAM play a minor role. Different basis sets were tried in combination with LSDA and BP86 exchange-correlation functional.

In general terms, this study provides a firm basis for determining molecular orientation within OEG-containing SAMs from a comparison of experimental and ab initio modeled RA spectra. The same strategy has been used to find the Euler angles for both the alkyl- and OEG portions in a related class of OEG-terminated and amide-bridged alkanethiolate SAMs.[17] The generated knowledge is undoubtedly expected to improve the understanding of issues related to stability, packing, and phase behavior of OEG SAMs. It may in the long run also contribute to an improved understanding regarding the mechanisms behind the interaction between proteins and OEG SAMs. More specific results are as follows.

All characteristic bands of the SAM RA spectrum in the fingerprint region, their relative position, intensity, and shape are reproduced by BP86 and MP2 single-molecule spectra (in a single-parameter Lorentzian description) with nearly one-to-one correspondence. The multimode structure is shown to be characteristic for the main COC band in the low frequency region. However, the multimode structure is not consistently represented by the different computational methods, and that was found to be a general drawback of our approach. In the CH-stretching region, the same methods and same model assumptions yield rather poor reproducibility of observed spectrum structure. First, all of the ab initio methods used misplace symmetric and in-plane asymmetric stretching vibrations of the CH_3 group attached to the oxygen. Second, the existing software does not allow the reliable estimate of spectral changes due to Fermi resonances and corresponding contribution of enhanced combination modes to infrared absorption. For these reasons, an accurate description of the shape of the RA spectrum requires development of far more sophisticated ab initio schemes.

Despite these limitations, comparison of simulated RA spectra in the CH-stretching region with relevant experimental data has proved instructive for our understanding of how and why particular vibrations reveal themselves in observed spectrum shape. As confirmed by this study, the dominating peak in the region at $\sim$2890 cm^{-1} represents asymmetric CH_2 stretching vibrations (principal result of our previous work[7]). The present analysis also suggests that the main-band high-frequency shoulder at $\sim$2920 cm^{-1} originates from one of two possible kinds of asymmetric CH_3 stretching vibrations. The most plausible mechanism that underlies the appearance of a low frequency shoulder at $\sim$2865 cm^{-1} seems to be a kind of Fermi-resonance between CH-stretching modes and one combined wagging+bending mode that is shown to have a suitable frequency. Hence, these are mostly CH_2^- vibrations that show up in the peak and low-frequency shoulder of the main band in the region. Symmetric CH_2 stretching vibrations make a minor contribution into the observed band. Earlier, the sidebands at 2816 and 2979 cm^{-1} were assigned, respectively, to symmetric and asymmetric vibrations of the CH_3 group.[3] That assignment is confirmed by present calculations with an increased insight into the nature of these bands.

The undertaken modeling combined with a wealth of relevant experimental data supports the following sequence of observed spectral modes (from lower to higher frequencies): combination twisting+bending mode (2744 cm^{-1}); mixed CH_3^+/CH_2^+ modes dominated by CH_3^+ vibrations (in close vicinity to the band at 2816 cm^{-1}); mostly CH_2^+ modes (2820−2860 cm^{-1}), which are almost hidden in RA spectra because of a perpendicular orientation with respect to the gold surface; predominantly CH_2^- modes (2860−2950 cm^{-1}) giving Fermi-resonance with combination vibrations at $\sim$2865 cm^{-1}; $CH_3^{(op)-}$ mode at $\sim$2920 cm^{-1}; $CH_3^{(ip)-}$ mode at 2979 cm^{-1}. To our knowledge, this is the first interpretation of *all* spectral features observed in CH-stretching region of ordered self-assemblies of $SH(EG)_nCH_3$. The suggested assignment can be of use for further refinement of details to elucidate the structure and properties of more complex OEG-terminated SAMs.

Acknowledgment. This work was supported by the Swedish Foundation for Strategic Research (SSF) through the Biomimetic Materials Science program, and by the Swedish Research Council (VR). The authors thank Dr. D. J. Vanderah for his data files of the reflection−absorption SAM spectra.

References and Notes

(1) Vanderah, D. J.; Arsenault, J.; La, H.; Gates, R. S.; Silin, V.; Meuse, C. W. *Langmuir* **2003**, *19*, 3752.
(2) Pale-Grosdemange, C.; Simon, E. S.; Prime, K. L.; Whitesides, G. M. *J. Am. Chem. Soc.* **1991**, *113*, 12.
(3) Harder, P.; Grunze, M.; Dahint, R.; Whitesides, G. M.; Laibinis, P. E. *J. Phys. Chem. B* **1998**, *102*, 426.
(4) Valiokas, R.; Östblom, M.; Svedhem, S.; Svensson, S. C. T.; Liedberg, B. *J. Phys. Chem. B* **2001**, *105*, 5459.
(5) Vanderah, D. J.; Valincius, G.; Meuse, C. W. *Langmuir* **2002**, *18*, 4674.
(6) Lang, H.; Duschl, C.; Vogel, H. *Langmuir* 1994, *10*, 197. Munro, J. C.; Frank, C. W.; *Langmuir* **2004**, *20*, 10567.
(7) Malysheva, L.; Klymenko, Yu.; Onipko, A.; Valiokas, R.; Liedberg, B.; *Chem. Phys. Lett.* **2003**, *370*, 451.
(8) Zolk, M.; Eisert, F.; Pipper, J.; Herrwerth, S.; Eck, W.; Buck, M.; Grunze, M. *Langmuir* **2000**, *16*, 5849.
(9) Dreesen, L.; Humbert, C.; Hollander, P.; Mani, A. A.; Ataka, K.; Thiry, P. A.; Peremans, A.; *Chem. Phys. Lett.* **2003**, *333*, 327.
(10) Miyazawa, T.; Fukushima, K.; Ideguchi, Y. *J. Chem. Phys.* **1962**, *37*, 2764.
(11) Kobayashi, M.; Sakashita, M. *J. Chem. Phys.* **1992**, *96*, 748.
(12) Gejji, S. P.; Tegenfeldt, J. Lindgren, J. *Chem. Phys. Lett.* **1994**, *226*, 427.
(13) Jaffee, R. L.; Smith, G. D.; D. Y. Yoon *J. Phys. Chem.* **1993**, *97*, 12745.
(14) Wang, R. L. C.; Kreuzer, H. J.; Grunze, M. *Phys. Chem. Chem. Phys.* **2000**, *2*, 3613.
(15) Buck, M. *Phys. Chem. Chem. Phys.* **2003**, *5*, 18.
(16) Parikh, A. N.; Allara, D. L. *J. Chem. Phys.* **1992**, *96*, 927.
(17) Malysheva, L.; Onipko, A.; Valiokas, R.; Liedberg, B. *Appl. Surf. Sci.*, available online, doi:10.1016/j.apsusc.2004.11.070.
(18) Ong, T. H.; Davies, P. B. *Langmuir* **1993**, *9*, 1836.
(19) Svedhem, S.; Hollander, S-Å.; Shi, J.; Konradsson, P.; Liedberg, B.; Svensson, S. C. T. *J. Org. Chem.* **2001**, *66*, 4494.
(20) Snyder, R. G.; Zerbi, G. *Spectrochim. Acta* **1967**, *23A*, 391.
(21) Allan, A.; McKean, D. C.; Perchard, J.-P.; Josien, M.-L. *Spectrochim. Acta* **1971**, *27A*, 1409.
(22) Matsuura, H.; Miyazawa, T.; Machida, K. *Spectrochim. Acta* **1973**, *29A*, 771.